ANALYSIS OF THE THERMAL PROPERTIES OF GaInAs QUANTUM CASCADE LASERS

ANÁLISIS DE LAS PROPIEDADES TÉRMICAS DE LÁSERES DE CASCADA CUÁNTICA DE GaInAs

O. Concepción[a], A. Abelenda[a], J. C. González[b] and M. Sánchez[a†]

a) Facultad de Física, Universidad de La Habana, Cuba. maruchy@fisica.uh.cu†
b) Dpto. de Física, Universidade Federal de Minas Gerais, Brasil.
† corresponding author

Received 16/12/2014; Accepted 18/03/2015

A study of the temperature distribution of GaInAs/AlInAs quantum cascade lasers (QCLs) is presented. The heat conduction equation was solved using a finite-element method and a two-dimensional anisotropic heat-flow model. The thermal resistance (R_{th}) was calculated and compared with experimental results reported by other authors obtaining a good agreement. Comparison of heat dissipation in a double channel (DC) and buried heterostructure (BH) was performed analyzing the influence of the ridge height. The effect of materials used as: heat-sink, capping and insulation layer were evaluated. The results show that a DC-QCL with a deep-ridge waveguide, using: InP as top capping layer, Si_3N_4 as insulation layer, and graphene as heat-sink presents a better performance than a BH-QCL.

Se presenta un estudio de la distribución de temperaturas en láseres de cascada cuántica (QCLs) de GaInAs/AlInAs. La ecuación de conducción del calor se resolvió por el método de los elementos finitos, utilizando un modelo anisotrópico y bidimensional del flujo de calor. Se calculó la resistencia térmica (R_{th}) y se comparó con resultados experimentales reportados por otros autores obteniéndose una buena concordancia. Se realiza una comparación entre las estructuras de doble canal (DC)y enterrada (BH), analizando la influencia de la altura del contacto. Se evaluó el efecto de los materiales usados como: disipador, capa de contacto y aislante. Los resultados muestran que un DC-QCL con un contacto profundo, usando: InP como capa de contacto superior, Si_3N_4 como óxido y grafeno como disipador tiene un mejor rendimiento que un BH-QCL.

PACS: Thermal analysis 81.70.Pg, Semiconductor lasers42.55. Px, ComputerModeling and simulation 07.05.Tp, Heat conduction 44.10.+i

I INTRODUCTION

Quantum cascade lasers are unipolar semiconductor devices based on intraband optical transitions. Unlike conventional interband laser diodes in which the emission wavelength is determined by the energy band gap, in QCLs the laser emission is achieved between quantized states whose energy difference can be engineered to obtain emission at different wavelengths using the same material system. Additionally, in a QCL, once an electron emits a photon, it remains in the conduction band and is injected into an adjacent identical stage in a cascading process allowing the emission of additional photons.

Since its experimental demonstration in 1994 [1], QCLs have experienced a fast development and are now established as viable light sources in the mid infrared (IR). InP based QCLs emitting at 4.9 *mu*m with output powers up to Watts in continuous-wave (CW), and very high wall plug efficiencies have been demonstrated [2] in the past years. However, compared with p-n lasers, QCLs exhibit considerably higher threshold currents and voltages, resulting in a more pronounced heating of the active region. Moreover, thermal dissipation in QCLs is very anisotropic being the component of the thermal conductivity in the direction perpendicular to the growth ($k_\perp$) much lower than the parallel component ($k_\parallel$) due to phonon reflections at the multiple interfaces in the growth direction.

Several processing techniques have been introduced to improve the heat dissipation in QCLs. One is the buried heterostructure [3] in which the active region is buried in a high thermal conductivity semiconductor material, facilitating the heat transfer from the active region in the lateral direction. However, this technique is complicated, time consuming and expensive since it requires an additional re-growth step. Another approach is the double-channel ridge waveguide. In this geometry, the waveguide in the lateral direction is delimited by two etched channels, followed by the deposition of a thick layer of gold to enhance the heat dissipation [4].

Therefore, device optimization focused on the improvement of heat dissipation is essential for obtaining more efficient QCLs, and for this purpose predictive simulation tools are extremely useful.

In this work we present a study of the temperature distribution and heat dissipation in GaInAs/AlInAs QCLs. The 2D heat conduction equation was solved using the finite-element method. With the values of the maximum active region temperature, the thermal resistance R_{th} was calculated and compared with reported experimental data obtaining a very good agreement. The two most used QCL designs were compared in terms of their influence on the increase of the active region temperature (ΔT) and possible optimizations are discussed. The effects of ridge depth and materials used as heat-sink, capping and electrical insulation

layer are investigated.

II DEVICE STRUCTURE AND THERMAL MODELING

The structure considered in the simulation is a double channel ridge waveguide GaInAs/AlInAs QCL emitting at wavelength of 6 μm as reported by Yu *et al.* [4]. The structure is composed of: the active core (injector/active region), waveguide, and cladding and cap layers. Thirty active/injector stages (~1.53 μm thick) were used as the emitting region and sandwiched between two 0.3 μm thick n-$Ga_{0.47}In_{0.53}As$ layers. The layer sequence for one stage is given in barrier/well pairs: (2.9/1.9), (2.6/2.0), (2.3/2.1), (2.2/2.3), (2.1/3.0), (2.1/4.2), (1.3/1.4), (5.0/1.4), (4.4/1.5), (3.9/2.4). The thicknesses are in nanometers. The well and barrier materials used are $Ga_{0.36}In_{0.64}As$ and $Al_{0.62}In_{0.38}As$, respectively. The upper cladding layer consists of a 2 μm thick n-InP, followed by a 1 μm thick n^+-$Ga_{0.47}In_{0.53}As$ capping layer. The device was grown onto an InP substrate which acts as a lower waveguide cladding layer. The 450 nm SiO_2 layer is used as isolation material to define the top contact and confine the injected current only to the active region. The ridge is 15 μm width and 5.13 μm deep, and a 5 μm-thick Au layer was electroplated around the laser ridges. Calculations were done for epilayer-side up mounted devices with a total width of 80 μm and 2000 μm of cavity length.

To obtain the temperature profile inside the QCL, the steady state heat flow equation was solved. Due to the device symmetry, the equation reduces to a two-dimensional form:

$$\nabla\cdot[k\nabla T(x,y)] + g(x,y) = 0. \quad (1)$$

Here $g(x,y)$ is the heat generated per unit volume (W/m^3), T is the temperature (K), and k is the thermal conductivity (Wm^{-1}K^{-1}).

Eq.(1) was solved using the finite-element method. The boundary conditions considered are the following:

(i) thermally isolated sidewalls;

(ii) no heat flow through the upper surface, because of the negligible effect of thermal radiation and thermal diffusion of air particles; considering the laser mounted epilayer-up, the upper surface is the outmost layer grown;

(iii) due to the high value of the thermal conductivity of the heat-sink and its much larger dimensions than those of the laser, it is assumed to remain at the ambient temperature;

(iv) the heat flow and the temperature are continuous at the interfaces between the laser layers.

Our heat-flow model takes into account two heat sources, the heat generated in the active region and resistive Joule heating in the rest of the layers. The power density in the active region is given by the equation $Q = V_{th}I_{th}/U$, where V_{th} is the threshold voltage, I_{th} is the threshold current, and U is the volume of the active core. In order to account for the anisotropy of the thermal conductivity in the active region, the values of the in-plane, $k_{\|}$ and cross-plane, $k_{\perp}$ components were taken from Refs. [5–7]. The rest of the layers were considered to be isotropic. Layers composing the injector and active region were considered separately, differing from the common practice to treat the whole active region as being just one material.

The structural parameters and thermal conductivities used in calculation are listed in Table 1. The thermal conductivity of the ternary and quaternary layers was obtained by interpolation from that of the corresponding binaries [8].

Table 1. Thermal conductivities and layer thicknesses of the structure simulated.

Material	Thickness (μm)	Thermal Conductivity (W/mK)
Heat sink/copper	400	398.36
Ti	0.04	21.6
Au	0.12	317.33
n-InP sustrate/cladding	89.26	68
n-$Ga_{0.47}In_{0.53}As$	0.3	4.82
$Ga_{0.36}In_{0.64}As/Al_{0.62}In_{0.38}As$	1.53	$k_{\|}$ = 5.5
active region (30 stages)		$k_{\perp}$ = 2.2
n-InP upper cladding	2	68
cap n^+-$Ga_{0.47}In_{0.53}As$	1	4.82
SiO_2	0.45	1.28

III RESULTS AND DISCUSSION

Figure 1 shows the temperature distribution profile in the growth direction for the DC-QCL described, epilayer-up onto a Cu heat-sink held at T= 300 K.

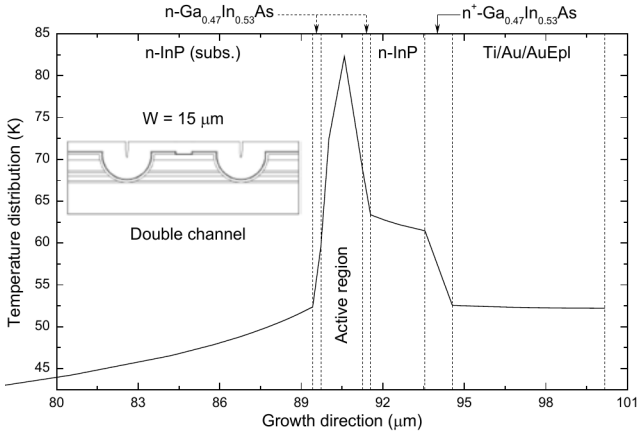

Figure 1. Calculated temperature distribution profile starting from the substrate. The inset schematically shows the cross section of the simulated device.

The operational parameters: threshold current density (J_{th} = 2.29 kA/cm^2), threshold voltage (V_{th} = 9.26 V) and device length (L = 2 mm) were taken from Ref. [4], corresponding to a power density $Q = 1.3810^{14}$ W/m^3.

In the simulation, the heat-sink temperature was kept at 300 K and the device is assumed to be epilayer-up mounted.

It is clear that in the epilayer-down bonding the heat dissipation is considerably improved because the active region is placed closer to the heat-sink. However, this scheme is more complicated due to the risk of a short circuit or contamination of the laser facet with the indium solder, and the epilayer-up mounting is generally preferred.

As can be seen in Figure 1, the maximum temperature is attained at the center of the active region, being ΔT= 82.3 K for a heat-sink temperature of 300 K. This is in very good agreement with the values of 79 K and 83.9 K obtained in Ref. [4] for heat-sink temperatures of 293 K and 308 K respectively. The heat generated in the active core transfers mainly via the InP substrate. Thus, the internal temperature becomes lower at the edges of the active region.

The thermal resistance is a parameter typically used to compare the thermal performance of the devices and can be obtained from the expression:

$$R_{th} = \frac{\Delta T}{J_{th} V_{th} A}, \tag{2}$$

where ΔT is the temperature difference between the active region and the heat sink and A is the area of the active region, that is the product of the ridge width W by the laser length.

According to Eq.(2) and using the value of ΔT= 82.3 K previously obtained, the thermal resistance is 12.9 K/W, which is in close agreement with the value of 13.2 K/W reported for this device at the heat sink temperature of 308 K [4].

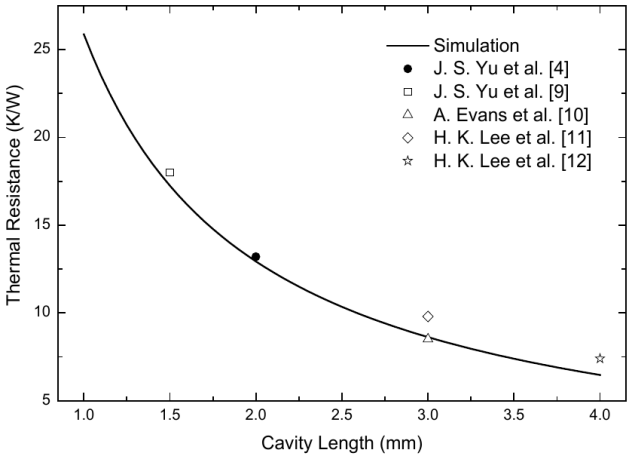

Figure 2. Cavity-length dependence of the thermal resistance for DC-QCLs. The solid line represents our calculation, and the circles, the experimental data reported in Refs. [9, 11, 12, 18].

In Figure 2 the calculated thermal resistance is plotted as a function of the cavity length (solid line). The black circle is the experimental value reported in Ref. [4] for the simulated device. For comparison, measured values reported for other DC-QCLs [9, 11, 12, 18] are also displayed.

As can be seen a very good agreement between our calculation and experimental reported data is obtained. It is important to point out the that solid line represents the R_{th} calculated for the structure modeled, which is not exactly the case of the other devices, thus differences between the model and real values are unavoidable.

To study the impact of the device geometry on the active region temperature, a comparison between a QCL sharing the same active region of the DC structure of Ref. [4], but having a buried waveguide, was done. In the simulation we have assumed that the two QCLs have the same injection current density (J_{th}= 2.29 kA/cm^2) and are epilayer-up bounded onto a heat-sink. The result obtained for the BH is ΔT = 78.2 K confirming that it is more efficient to remove the heat from the active region compared to the DC structure.

To optimize the DC structure to achieve results similar or better than the BH, the influence of the ridge height was analyzed. This is important since, in fabrication of the top contact, the ridges are etched to different depths, and often authors do not report the value of this important parameter. For instance, in Ref. [13] the ridge was etched down to approximately half of the lower cladding layer in a BH- QCL. In Ref. [14] the ridge was etched until 7 μm and in Ref. [3] 1 μm deep into the substrate.

Figure 3 shows the maximum temperature increase obtained in the active region as a function of the ridge height (h). Here h_1 corresponds to an etching depth where only the n$^+$-$Ga_{0.47}In_{0.53}As$ capping layer is removed (shallow-ridge waveguide). This procedure was repeated removing layer by layer. Thus h_2 is the case when both the n$^+$ capping and the top InP cladding layer are removed. Likewise, h_3 represents the case where all the layers above the active region are removed and h_4 when the whole active region is also eliminated, h_5 is the case in which the lower $Ga_{0.47}In_{0.53}As$ waveguide layer is also removed (deep-ridge waveguide), h_6 is the case in which a layer of 1 μm thickness from the substrate was removed.

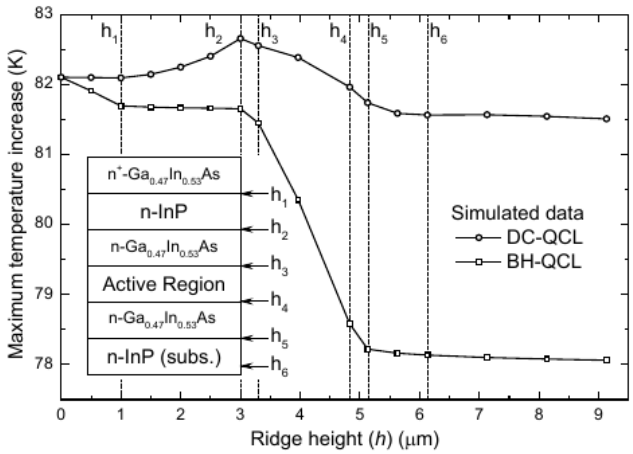

Figure 3. Calculated maximum temperature increase (ΔT) in the active region for the DC and BH QCL as a function of the ridge height (h).

It is clearly seen that the value of h plays an important role on the active region temperature being more pronounced in case of the BH. At first, the temperature rises as the depth is increased, reaches a maximum for a ridge depth h_2 and decreases thereafter. This result can be explained because with the elimination of the 2 μm InP cladding layer of high thermal conductivity the effective area to remove the heat is reduced. From this point on, a further increase in depth produces a successive decrease of the temperature, until it

reaches the substrate. This is because in this case the layers eliminated ($Ga_{0.47}In_{0.53}As$ and the active region) are very thin and have very low thermal conductivities. However, at the same time the active region is being surrounded by a thick layer of gold with a high thermal conductivity. Once the whole active region is etched out and both sides of the ridge are covered by gold, the lateral heat flux is enhanced.

The effect is more pronounced in the BH structure because in this case, as the etching depth is increased, the active region is getting more and more surrounded by a high thermal conductivity semiconductor material instead of the standard insulator/metal sidewall coverage used in DC structures. However, as mentioned previously, the BH is most complicated and expensive, since it requires an additional growing step.

According to these results, the optimum height, h_6, is that in which the ridge was etched a little into the substrate (~ 1 μm).

Note that, for depths greater than h_6 the temperature remains almost constant. This is because once both sides of the active region are covered by gold, the heat dissipation cannot be further improved since an additional increase in the etch depth no longer produces a significant increase in the effective area to remove the heat.

The effect of the material used as heat-sink was also evaluated. Copper is the standard heat sink used in almost all laser diode packages, owing to its excellent thermal conductivity, and its good mechanical machining properties. However, materials with even higher thermal conductivities are desired and we compared three different materials: copper (398.36 $Wm^{-1}K^{-1}$) [12], diamond (2000 $Wm^{-1}K^{-1}$) [15] and graphene (5000 $Wm^{-1}K^{-1}$) [16]. Figure 4 shows simulation results for a DC-QCL.

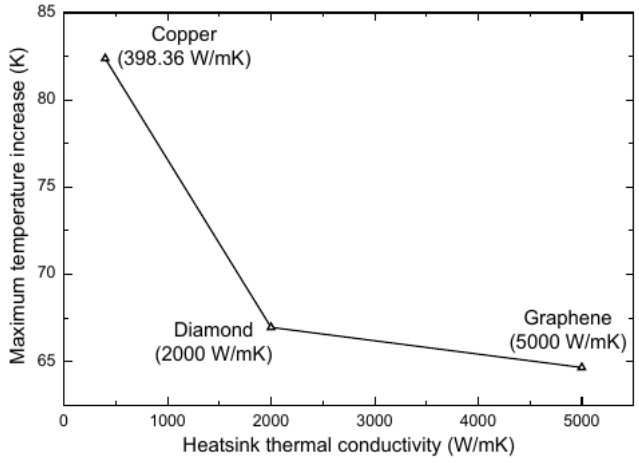

Figure 4. Dependence of maximum temperature on the thermal conductivity of the heat-sink. Results are shown for a DC-QCL epilayer-up mounted.

We included graphene in the comparison since it exhibits an extremely high thermal conductivity, among the highest of any known materials. It is important to note that the conductivity of graphene decreases significantly when it is in contact with a substrate, so there are still many technical challenges before graphene becomes industrially viable, however, this material holds an enormous potential for thermal management applications in future devices [17,18].

As expected the smallest increase in the temperature is obtained when graphene is used as a heat-sink. Compared with copper, a reduction of 21.4% in the active region temperature of the DC-QCL can be obtained.

Simulations were also done using Si_3N_4 as the insulator layer used to define the upper contact instead of SiO_2, and substituting the n^+-$Ga_{0.47}In_{0.53}As$ cap layer for InP. Silicon nitride has higher thermal conductivity (3.5 $Wm^{-1}K^{-1}$) than SiO_2 and besides a thermal expansion coefficient (CTE) of 3.3×10^{-6} K^{-1} [19], which is closer to the CTE of the semiconductor materials forming the structure. On the other hand, InP has a thermal conductivity about 15 times greater than the ternary GaInAs. Table 2 shows the value of maximum temperature in the device reported in Ref. [4], and the value predicted by the simulation when some parameters are optimized.

Table 2. Optimized parameters obtained from simulation.

Parameters	DC QCL ΔT (K)
SiO_2 as insulater layer. n^+-GaInAs cupper-heat-sink h_5	82.3
Si_3N_4 as insulater layer. n^+-InP graphene-heat-sink h_6	59.5

Results show that, with a ridge height h_6 equivalent to an etching deep of about 1 μm inside the substrate, replacing the SiO_2 isolation layer by Si_3N_4, and the n^+-$Ga_{0.47}In_{0.53}As$ capping layer by InP, and using graphene as heat-sink, the active region temperature of DC-QCLs can be reduced from 82.3 K to 59.5 K. This value is lower than the one obtained for the original BH, ΔT= 78.2 K proving that with a proper design the DC structure can be a good substitute for a more complex and expensive BH.

It is worthwhile noting to note that the performance of the double channel structure can be further improved by optimizing other parameters like the distance between channels. Moreover, a study of the combined effect of the geometrical parameters could give more insight to get the full optimization of the DC QCL from a thermal standpoint.

CONCLUSIONS

A comparison between the thermal behavior of DC and BH QCL is presented analyzing the influence of the different design parameters and materials on the active region temperature. Results show that with a proper design, the DC structure show better performance that the BH. An optimized ridge structure using: InP as top capping layer, Si_3N_4 combined with a deep-ridge waveguide is found to offer the best performance compared with the BH. To further optimize the QCL structures, the use of graphene as a heat-sink is recommended.

The authors would like to thank for the partial financial support of the Brazilian agency CAPES.

[1] J. Faist, F. Capasso, D. L. Sivco, C. Sirtori, A. L. Hutchinson and A. Y. Cho, Science **264**, 553 (1994).

[2] Y. Bai, N. Bandyopadhyay, S. Tsao, S. Slivken and M. Razeghi, Appl. Phys. Lett. **98**, 181102 (2011).

[3] M. Beck, J. Faist, C. Gmachl, F. Capasso, D. Sivco, J. Bailargeon and A. Y. Cho, Proc. SPIE **3284**, 231 (1998).

[4] J. S. Yu, S. Slivken, A. Evans, L. Dorisand M. Razeghi, Appl. Phys. Lett. **83**, 2503 (2003).

[5] G. M. de Naurois, B.Simozrag, G. Maisons, V. Trinite, F. Alexandreand M. Carras, Appl. Phys. Lett. **101**, 041113 (2012).

[6] K. Pierscinski, D. Pierscinska, M. Iwinska, K. Kosiel, A. Szerling, P. Karbownik and M. Bugajski, J. Appl. Phys. **112**, 043112 (2012).

[7] H. Lee and J. S. Yu, Solid-State Electronics **54**, 769 (2010).

[8] S. Adachi, J. Appl. Phys. **102**, 063501 (2007).

[9] J. S. Yu, A. Evans, J. David, L. Doris, S. Slivken and M. Razeghi, IEEE **16**, 747 (2004).

[10] A. Evans, J. Nguyen, S. Slivken, J. S. Yu,S. R. Darvish and M. Razeghi, Appl. Phys. Lett. **88**, 051105 (2006).

[11] H. K. Lee, K. S. Chung and J. S. Yu, Appl. Phys. B **93**, 779 (2008).

[12] H. K. Lee and J. S. Yu, Appl. Phys. B **106**, 619 (2012).

[13] L. Diehla, D. Bour, S. Corzine, J. Zhu, G. Hfler, M. Lonar, M. Troccoli and F. Capasso, Appl. Phys. Lett. **89**, 081101 (2006).

[14] M.Razeghi, IEEE J. Quantum Elect **15**, 941(2009).

[15] C. A. Evans, "The optical and thermal properties of quantum cascade laser", Ph.D. thesis, University of Leeds, 2008.

[16] A. A. Balandin, S. Ghosh, W. Bao, I. Calizo, D. Teweldebrhan, F. Miao and C. Ning Lau, Nano Lett. **8**, 902 (2008).

[17] S. Ghosh, I. Calizo, D. Teweldebrhan, E. P. Pokatilov, D. L. Nika, A. A. Balandin, W. Bao, F. Miao and C. N. Lau, Appl. Phys. Lett. **92**, 151911 (2008).

[18] N. Han et al., Nat. Commun. **4**, 1452 (2013).

[19] V. V. Mamutin, N. D. Ilyinskaya, D. A. Bedarev, R. V. Levin, and B. V. Pushnyi, Semiconductors **48**, 1103(2014).